Supplementary Material: Spectroscopy and Thermometry of Drumhead Modes in a Mesoscopic Trapped-Ion Crystal using Entanglement

Brian C. Sawyer,[1,*] Joseph W. Britton,[1] Adam C. Keith,[2,†] C.-C. Joseph Wang,[2]
James K. Freericks,[2] Hermann Uys,[3] Michael J. Biercuk,[4] and John J. Bollinger[1]

[1] *Time and Frequency Division, National Institute of Standards and Technology, Boulder, CO 80305*
[2] *Department of Physics, Georgetown University, Washington, DC 20057*
[3] *Council for Scientific and Industrial Research, Pretoria, South Africa*
[4] *Centre for Engineering Quantum Systems, School of Physics, The University of Sydney, NSW Australia*

I. OPTICAL DIPOLE FORCE DETAILS

Figure 1 shows a simple sketch of the optical dipole force (ODF) laser beam set-up. As discussed below, the frequency as well as the beam polarizations were chosen to null the AC Stark shift from an individual beam and to produce a state-dependent force which is equal in magnitude but opposite in sign for the $|\uparrow\rangle$ and $|\downarrow\rangle$ qubit states ($F_\uparrow = -F_\downarrow$). The off-resonant laser beam frequency was detuned from the cycling transition $\left(|\uparrow\rangle \rightarrow \left|P_{3/2}, m_J = 3/2\right\rangle\right)$ by $\Delta_R \simeq -63.8$ GHz. This gives detunings of 15.6 GHz and -26.1 GHz respectively from the $|\uparrow\rangle \rightarrow \left|P_{3/2}, m_J = 1/2\right\rangle$ and $|\downarrow\rangle \rightarrow \left|P_{3/2}, m_J = -1/2\right\rangle$ transitions. Laser beam waists were $w_z \simeq 100\ \mu$m in the vertical (z-direction) and $w_x \simeq 1$ mm in the horizontal direction. Here we define the waist as the distance from the center of the beam over which the electric field intensity decreases by $1/e^2$ (i.e. $I(z) \sim e^{-(z/w_z)^2}$). With the small 2.4^o incident angle each beam makes with respect to the plane of the crystal, this provided greater than 90% uniform electric field intensity across ion crystal arrays with $N < 250$.

We used linearly polarized laser beams. Let

$$\begin{aligned} \vec{E}_U(\vec{r},t) &= \hat{\epsilon}_U E_U \cos\left(\vec{k}_U \cdot \vec{r} - \omega_U t\right) \\ \vec{E}_L(\vec{r},t) &= \hat{\epsilon}_L E_L \cos\left(\vec{k}_L \cdot \vec{r} - \omega_L t\right) \end{aligned}$$

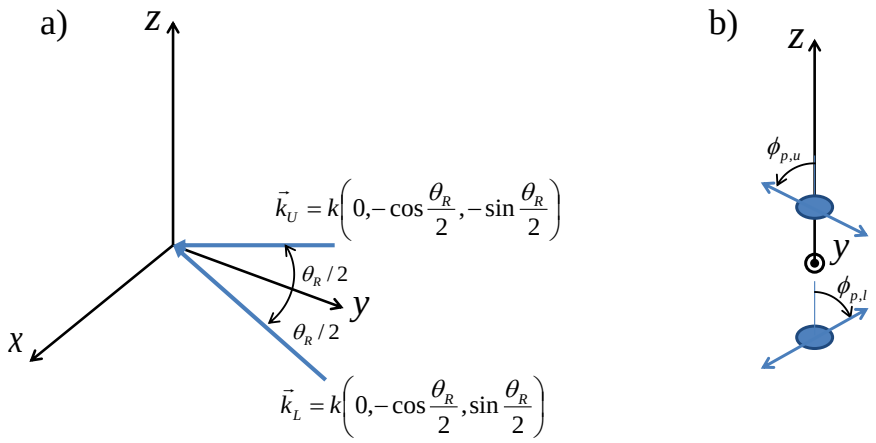

FIG. 1: Sketch of ODF laser beam setup. a) The ODF laser beams lie in the y-z plane at angles $\pm\theta_R/2$ with respect to the y-axis. b) View looking in the $-\hat{y}$ direction. The beams are linearly polarized but with different polarization angles relative to vertical polarization.

*Electronic address: brian.sawyer@boulder.nist.gov
†Department of Physics, North Carolina State University, Raleigh, NC 27695

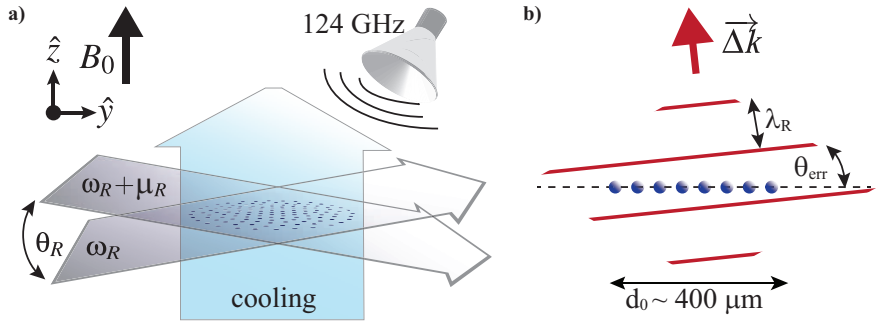

FIG. 2: (a) Sketch of the experimental setup showing a single-plane ion array, the optical dipole force laser beams which cross with an angle of θ_R at the ion array, and the main Doppler laser cooling beam which is directed along the magnetic field. Microwaves used to rotate the ion spins are introduced with a horn. (b) Sketch of the 1D optical lattice wave fronts (red lines) generated by the ODF laser beams. These wave fronts need to be aligned with the ion planar array (represented by the blue dots). Here $\lambda_R = 2\pi/|\overrightarrow{\Delta k}| \approx 3.7\,\mu$m and θ_{err} denotes the angle of misalignment. $d_0 \sim 400\,\mu$m is the typical array diameter for $N \sim 200$ ions. With the wave front alignment technique discussed in the text we obtain $\theta_{\rm err} < 0.05^\circ$.

denote the electric fields of the upper and lower ODF beams. If ϕ_p is the angle of the laser beam electric-field polarization with respect to vertical polarization ($\hat{\epsilon}\cdot\hat{x}=0$), then the AC Stark shift of the qubit states when illuminated by a single beam can be written

$$\begin{aligned}\Delta_{\uparrow,\,acss} &= A_\uparrow \cos^2(\phi_p) + B_\uparrow \sin^2(\phi_p)\\ \Delta_{\downarrow,\,acss} &= A_\downarrow \cos^2(\phi_p) + B_\downarrow \sin^2(\phi_p)\end{aligned}$$

where $A_\uparrow(A_\downarrow)$ is the Stark shift of the $|\uparrow\rangle(|\downarrow\rangle)$ state for a π-polarized beam ($\hat{\epsilon}$ parallel to the $\hat{z}$-axis) and $B_\uparrow(B_\downarrow)$ is the Stark shift of the $|\uparrow\rangle(|\downarrow\rangle)$ state for a σ-polarized beam ($\hat{\epsilon}$ perpendicular to the $\hat{z}$-axis). (Here we neglect the small σ polarization ($\propto \sin(2.4^o)$) that exists when $\phi_p = 0$.) The Stark shift of the qubit transition is

$$\Delta_{acss} = (A_\uparrow - A_\downarrow)\cos^2(\phi_p) + (B_\uparrow - B_\downarrow)\sin^2(\phi_p)\ . \tag{1}$$

If $A_\uparrow - A_\downarrow$ and $B_\uparrow - B_\downarrow$ have opposite signs, there is an angle which makes $\Delta_{acss} = 0$. For a laser detuning of $\Delta_R = -63.8$ GHz, $\Delta_{acss} = 0$ at $\phi_p \simeq \pm 65^o$.

With $\Delta_{acss} = 0$ for each ODF laser beam, we exploit the freedom to choose their polarization in order to obtain a state-dependent force. Specifically we choose $\vec{E}_U$ to have a polarization given by $\phi_{p,u} = 65^o$ and $\vec{E}_L$ to have a polarization given by $\phi_{p,l} = -65^o$. In this case the interference term in the expression for the electric field intensity $\left(\vec{E}_U + \vec{E}_L\right)^2$ produces a polarization gradient which results in spatially dependent AC Stark shifts

$$\begin{aligned}&\left(A_\uparrow \cos^2(\phi_p) - B_\uparrow \sin^2(\phi_p)\right) 2\cos(\delta k\cdot z - \mu_R t)\\ &\left(A_\downarrow \cos^2(\phi_p) - B_\downarrow \sin^2(\phi_p)\right) 2\cos(\delta k\cdot z - \mu_R t)\end{aligned}$$

for the qubit levels. Here $\delta k \equiv \left|\vec{k}_U - \vec{k}_L\right| = 2k\sin\left(\frac{\theta_R}{2}\right)$ is the wave vector difference between the two ODF laser beams, $\mu_R = \omega_U - \omega_L$ is the ODF beat note, and $\phi_p = |\phi_{p,u}| = |\phi_{p,l}|$. The spatially dependent AC Stark shift produces a state-dependent force $F_{\uparrow,\downarrow}(z,t) = F_{\uparrow,\downarrow}\sin(\delta k\cdot z - \mu_R t)$ where

$$\begin{aligned}F_\uparrow &= 2\,\delta k\left(A_\uparrow \cos^2(\phi_p) - B_\uparrow \sin^2(\phi_p)\right)\\ F_\downarrow &= 2\,\delta k\left(A_\downarrow \cos^2(\phi_p) - B_\downarrow \sin^2(\phi_p)\right)\end{aligned}\ .$$

In general $F_\uparrow \neq -F_\downarrow$. We operate at $\Delta_R = -63.8$ GHz where for $\Delta_{acss} = 0$ we also obtain $F_\uparrow = -F_\downarrow \equiv F$.

For a given $\phi_{p,u}$, $\phi_{p,l}$, and Δ_R we use straight forward atomic physics along with well known values for the energy levels and matrix elements of $^9Be^+$ to calculate F as a function of the electric field intensity $I_R = \frac{c\epsilon_o}{2}|E_L|^2 = \frac{c\epsilon_o}{2}|E_U|^2$ at the center of the laser beams. For $\theta_R = 4.8^o$ and $I_R = 1$ W/cm^2 , we obtain $F = 1.5\times10^{-23}$ N.

II. WAVE FRONT ALIGNMENT

The ODF laser beams produce a 1D optical lattice characterized by the effective wave vector $\delta\vec{k}$ and beat note μ_R. In the previous section we assumed that $\delta\vec{k} \parallel \hat{z}$, or equivalently that the wave fronts of the lattice were aligned

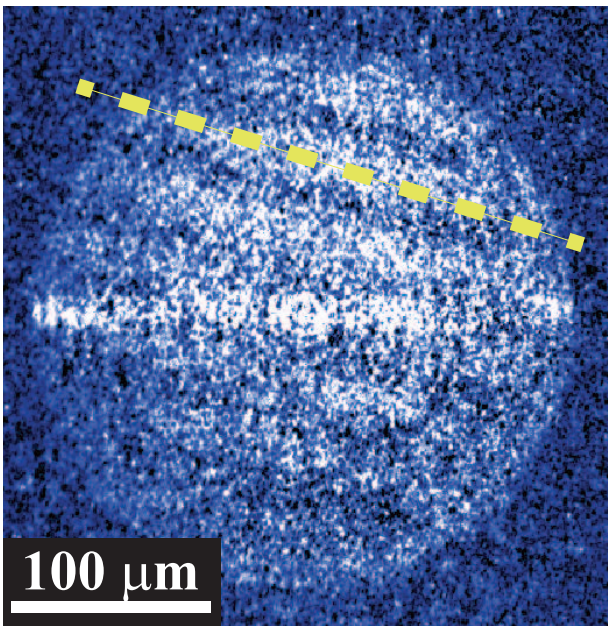

FIG. 3: Top-view image of the spatially inhomogeneous fluorescence from a single ion plane produced by the AC Stark from a static ($\mu_R = 0$) optical dipole force lattice with misaligned wave fronts. Dark bands are regions of high standing wave electric field intensity (parallel to the dashed yellow line). The bright horizontal feature bisecting the center of the image is fluorescence from the weak Doppler laser cooling beam directed perpendicular to the magnetic field. The image was obtained by subtracting a background image with the ODF beams off.

perpendicular to the $\hat{z}$-axis (magnetic field axis). If the wave fronts are not normal to the $\hat{z}$-axis as sketched in Fig. 2, then the time dependence of the optical dipole force seen by an ion in the rotating frame depends on the (x, y) position of the ion. This complicates the interaction generated by the optical dipole force and is avoided by careful alignment.

We used top-view images (images of the ion resonance fluorescence scattered along the magnetic field) from a single plane to measure a misalignment of the ODF wave fronts. For this measurement we set $\mu_R = 0$ (stationary 1D lattice) and detune the frequency of the ODF laser beams approximately 0.5 GHz below the $|\uparrow\rangle \rightarrow \left|^2P_{3/2}\, m_J = +3/2\right\rangle$ Doppler cooling transition. This small detuning generates sufficiently large AC Stark shifts on the cooling transition to measurably change the ion scatter rate from the Doppler cooling laser. With the Doppler cooling laser on and the ODF beams turned off we observe a spatially uniform, time-averaged image of a rotating planar crystal. With the ODF beams on, ions located in regions of high electric field intensity at the anti-nodes of the optical lattice are Stark shifted out of resonance with the Doppler cooling laser. This is what produced the dark bands in the top-view image shown in Fig. 3. From images like this we determine how to move the ODF beams to align the wave fronts normal to $\hat{z}$. Improved alignment is indicated by a longer wavelength fringe pattern. With this technique we have aligned the ODF wave fronts with the planar array to better than $\theta_{err} \lesssim 0.05^o$.

Images like that shown in Fig. 3 were typically obtained with 1 s integration. This means the imprint of the 1D lattice on the planar arrays was stable during the integration time and indicates a phase stability of our 1D lattice of better than 1 s. We note that direct fluorescence imaging of the 1D lattice, for example by tuning the ODF laser resonant with the Doppler cooling transition, is not viable. Even at low powers, resonantly scattered photons across the large horizontal waist of the ODF beams apply a large torque, causing the rotation frequency and radius of the array to rapidly change, typically driving the ions into very large radial orbits.

III. SPIN-MOTION ENTANGLEMENT PRODUCED BY THE SPIN-DEPENDENT OPTICAL DIPOLE FORCE

With the wave vector $\delta\vec{k}$ of the 1D optical lattice aligned parallel to $\hat{z}$, the optical dipole force generated by the lattice is independent of the ion position and can be written

$$F_{\uparrow}(t) = -F_{\downarrow}(t) \equiv F\cos\left(\mu_R t\right) \tag{2}$$

where μ_R is the frequency difference between the ODF laser beams. More generally we allow for the possibility that the ODF laser intensity could be diferent for each ion, resulting in a different spin-dependent force F_j for each ion j,

$$F_{j\uparrow}(t) = -F_{j\downarrow}(t) \equiv F_j \cos(\mu_R t) \ . \tag{3}$$

In the experimental set-up, the variation in F_j is less than 20%. The ODF interaction with the ion spins can be written as

$$H_{ODF} = -\sum_{j=1}^{N} F_j \cos(\mu_R t)\, \hat{z}_j \hat{\sigma}_j^z \ . \tag{4}$$

Here $\hat{z}_j$ is the axial position operator for the j^{th} ion, which can be written in terms of the axial normal modes $\left(\vec{b}_m, \omega_m\right)$ of the planar array,

$$\hat{z}_j = \sum_{m=1}^{N} b_{jm} \sqrt{\frac{\hbar}{2M\omega_m}} \left(\hat{a}_m e^{-i\omega_m t} + \hat{a}_m^\dagger e^{i\omega_m t}\right) \ . \tag{5}$$

The eigenvectors are normalized so that $\sum_m |b_{jm}|^2 = \sum_j |b_{jm}|^2 = 1$. Both the eigenvectors $\vec{b}_m$ and eigenfrequencies ω_m are calculated by solving for the ion equilibrium positions and diagonalizing the stiffness matrix obtained by Taylor expansion of the potential about the ion equilibrium positions [1].

The Hamiltonian H_{ODF} of Eq. (4) is time dependent. The evolution operator for H_{ODF} is obtained from a second order expansion of the Magnus formula [2, 3]

$$\hat{U}_{ODF}(t) = \exp\left[\frac{-i}{\hbar}\int_0^t H_{ODF}(t')dt' - \frac{1}{2\hbar^2}\int_0^t dt_2 \int_0^{t_2} \left[H_{ODF}(t_2), H_{ODF}(t_1)\right] dt_1\right] \ . \tag{6}$$

Higher order terms do not contribute as the commutator $[H_{ODF}(t_2), H_{ODF}(t_1)]$ commutes with $H_{ODF}(t')$. Following the discussion of Ref. [3], $U_{ODF}(t)$ can be written

$$\begin{aligned} \hat{U}_{ODF}(t) &= \exp\left[\sum_j \left(\sum_m \left(\alpha_{jm}(t)\hat{a}_m^\dagger - \alpha_{jm}^*(t)\hat{a}_m\right)\hat{\sigma}_j^z\right) + i\sum_{j,k} J_{j,k}(t)\hat{\sigma}_j^z\hat{\sigma}_k^z\right] \\ &= \exp\left[\sum_j \left(\sum_m \left(\alpha_{jm}(t)\hat{a}_m^\dagger - \alpha_{jm}^*(t)\hat{a}_m\right)\hat{\sigma}_j^z\right)\right] \cdot \exp\left[i\sum_{j,k} J_{j,k}(t)\hat{\sigma}_j^z\hat{\sigma}_k^z\right] \ . \\ &\equiv \hat{U}_{SM}(t)\cdot\hat{U}_{SS}(t) \end{aligned} \tag{7}$$

The first term $U_{SM}(t)$ describes spin-dependent displacements $\alpha_{jm}(t)$ of the normal modes m where, for the $\cos(\mu_R t)$ time dependence of the interaction in Eq. (4),

$$\alpha_{jm}(t) = \frac{F_j b_{jm} z_{0m}}{\hbar\left(\mu_R^2 - \omega_m^2\right)}\left[\omega_m - e^{i\omega_m t}\left(\omega_m\cos(\mu_R t) - i\mu_R \sin(\mu_R t)\right)\right] \ . \tag{8}$$

Here $z_{0m} = \sqrt{\hbar/(2M\omega_m)}$. The second term $\hat{U}_{SS}(t)$ describes an effective spin-spin interaction where the pairwise coupling $J_{j,k}(t)$ is given by

$$J_{j,k}(t) = \frac{F_j F_k}{2\hbar^2}\sum_m \frac{b_{jm}b_{km}z_{0m}^2}{\mu_R^2 - \omega_m^2}\left\{\frac{\omega_m \sin(\mu_R - \omega_m)t}{\mu_R - \omega_m} + \frac{\omega_m \sin(\mu_R + \omega_m)t}{\mu_R + \omega_m} - \frac{\omega_m \sin(2\mu_R t)}{2\mu_R} - \omega_m t\right\} \ . \tag{9}$$

For now we assume $\hat{U}_{SS}(t)$ can be neglected. We will discuss the validity of this assumption at the end of this section.

The interaction $\hat{U}_{SM}(t) = \exp\left[\sum_j \left(\sum_m \left(\alpha_{jm}(t)\hat{a}_m^\dagger - \alpha_{jm}^*(t)\hat{a}_m\right)\hat{\sigma}_j^z\right)\right]$ generates spin-motion entanglement that is the subject of this study. The commutator

$$\begin{aligned} \left[\alpha_{jm}(t)\hat{a}_m^\dagger - \alpha_{jm}^*(t)\hat{a}_m, \alpha_{km}(t)\hat{a}_m^\dagger - \alpha_{km}^*(t)\hat{a}_m\right] &= \alpha_{jm}(t)\alpha_{km}^*(t) - \alpha_{jm}^*(t)\alpha_{km}(t) \\ &= 0 \end{aligned}$$

because $\alpha_{jm}(t)\alpha_{km}^*(t)$ is real. Therefore we can write $\hat{U}_{SM}(t)$ as a product of individual spin displacements

$$\hat{U}_{SM}(t) = \prod_{j,m} \exp\left(\left(\alpha_{jm}(t)\hat{a}_m^\dagger - \alpha_{jm}^*(t)\hat{a}_m\right)\hat{\sigma}_j^z\right) \ . \tag{10}$$

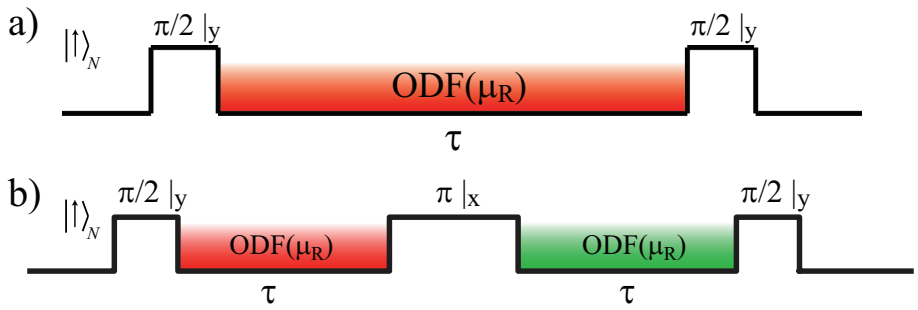

FIG. 4: Pulse sequences described in this supplemental material. a) Ramsey pulse sequence consisting of two $\pi/2$ rotations with an intermediate arm of duration τ during which the ODF is applied. b) The spin echo sequence repeated from Fig. 2(a) of the Letter which consists of two arms of duration τ.

By neglecting the spin-spin entanglement ($\hat{U}_{SS}(t)$) we can independently calculate the evolution of each spin j.

We now calculate the spin motion entanglement generated by $\hat{U}_{SM}(t)$ during the free precession period of a Ramsey sequence shown in Fig. 4(a). The calculation for the spin-echo sequence of Fig. 4(b) used in the experiments is identical except for a more complicated expression for the $\alpha_{jm}(t)'$s (see next section). Each spin j is prepared in state $|\uparrow\rangle$ at the start of the sequence. If an ODF is not applied during the free precession period, the spin is rotated to the dark $|\downarrow\rangle$ state by the final $\pi/2$ pulse of the sequence. With the application of a spin-dependent ODF, in general the spin is entangled with the motion at the end of the Ramsey sequence. We detect this spin-motion entanglement by measuring the probability of finding spin j in the $|\uparrow\rangle$ state. Let

$$\hat{U}^{(j)}_{SM}(t) = \exp\left(\sum_m \left(\alpha_{jm}(t)\hat{a}^\dagger_m - \alpha^*_{jm}(t)\hat{a}_m\right)\hat{\sigma}^z_j\right)$$

denote the evolution of spin j by the spin-dependent ODF. By re-writing

$$\hat{U}^{(j)}_{SM}(t) = \cosh\left(\sum_m \left(\alpha_{jm}\hat{a}^\dagger_m - \alpha^*_{jm}\hat{a}_m\right)\right) + \sinh\left(\sum_m \left(\alpha_{jm}\hat{a}^\dagger_m - \alpha^*_{jm}\hat{a}_m\right)\right)\hat{\sigma}^z_j$$

we calculate

$$P^{(j)}_{\uparrow,SM} = \left\langle \left(\sinh\left(\sum_m \left(\alpha_{jm}\hat{a}^\dagger_m - \alpha^*_{jm}\hat{a}_m\right)\right)\right)^\dagger \sinh\left(\sum_m \left(\alpha_{jm}\hat{a}^\dagger_m - \alpha^*_{jm}\hat{a}_m\right)\right)\right\rangle_{th} \tag{11}$$

where $P^{(j)}_{\uparrow,SM}$ denotes the probability of measuring the $|\uparrow\rangle$ state for spin j produced by the $\hat{U}_{SM}(t)$ interaction, and $\langle\,\rangle_{th}$ denotes an expectation value averaged over a thermal (Maxwell-Boltzmann) distribution of modes. We evaluate Eq. (11) by writing the sinh functions in exponential form. It is then necessary to evaluate expressions of the form $\left\langle e^{\hat{A}}e^{\hat{B}}\right\rangle_{th}$ where $\hat{A}$ and $\hat{B}$ are operators which are linear in the raising and lowering operators $\hat{a}^\dagger_m$ and $\hat{a}_m$. In this case we can make use of the result [4]

$$\left\langle e^{\hat{A}}e^{\hat{B}}\right\rangle_{th} = e^{(1/2)\left\langle \hat{A}^2+2\hat{A}\hat{B}+\hat{B}^2\right\rangle_{th}}$$

to obtain

$$P^{(j)}_{\uparrow,SM} = \frac{1}{2}\left[1 - \exp\left(-2\sum_m |\alpha_{jm}(t)|^2\left(2\bar{n}_m+1\right)\right)\right]. \tag{12}$$

Here $\bar{n}_m \simeq k_B T_m/(\hbar\omega_m)$ is the mean occupation number of a Maxwell-Boltzmann distribution characterized by temperature T_m. We measure the probability of detecting $|\uparrow\rangle$ averaged over all the ions $\left(\sum_j P^{(j)}_\uparrow\right)/N$.

The simple result of Eq. (12) was obtained under the assumption that we could neglect $\hat{U}_{SS}(t)$ in Eq. (7). In general $\hat{U}_{SS}(t)$ will contribute to the measured $P^{(j)}_\uparrow$. This can be straight forwardly estimated when μ_R is tuned close to the

COM mode ω_1. In this case the resulting pair-wise interaction coefficients are identical for all ion pairs $J_{j,k}(t) \simeq J(t)$ with

$$J(t) = \frac{F^2}{2\hbar^2} \cdot \frac{z_{01}^2}{N\left(\mu_R^2 - \omega_1^2\right)} \left\{ \frac{\omega_1 \sin(\mu_R - \omega_1)t}{\mu_R - \omega_1} + \frac{\omega_1 \sin(\mu_R + \omega_1)t}{\mu_R + \omega_1} - \frac{\omega_1 sin(2\mu_R t)}{2\mu_R} - \omega_1 t \right\} .$$

For small detunings $|\mu_R - \omega_1| \ll \omega_1$, $J(t)$ is approximately bounded by $|J(t)| \lesssim J \cdot t$ where

$$J = \frac{F^2}{2\hbar^2} \cdot \frac{z_{01}^2}{N\left(\mu_R^2 - \omega_1^2\right)} \omega_1 .$$

The fully connected, uniform Ising interaction $\exp\left[iJ\left(\sum_{j,k} \hat{\sigma}_j^z \hat{\sigma}_k^z\right)t\right]$ obtained by coupling through the COM mode is identical to the single-axis twisting interaction analyzed by Kitagawa and Ueda [5]. We use the expressions given in Ref. [5] to calculate $P_{\uparrow,SS}^{(j)}$, the probability of measuring spin j in the $|\uparrow\rangle$ state at the end of the Ramsey sequence due to the $\hat{U}_{SS}(t)$ interaction,

$$P_{\uparrow,SS}^{(j)} \simeq \frac{1}{2}\left[N 8 (Jt)^2\right] . \tag{13}$$

This expression is valid for short times t where $P_{\uparrow,SS}^{(j)}$ is small.

We obtain strong spin-motion entanglement for small detunings $|\mu_R - \omega_1| \ll \omega_1$. The magnitude of the coherently driven amplitude $\alpha_{j,m=1}(t)$ in the expression for $\hat{U}_{SM}(t)$ (Eq. (10)) and $P_{\uparrow,SM}^{(j)}$ (Eq. (12)) is maximized for a detuning $|\mu - \omega_1| \simeq \pi/t$ where

$$|\alpha_{j,1}|_{max} = \left|\alpha_{j,1}\left(t \simeq \frac{\pi}{|\mu_R - \omega_1|}\right)\right| \simeq \frac{F z_{01}}{\hbar\sqrt{N}\left|\mu_R^2 - \omega_1^2\right|} 2\omega_1 .$$

The above expression neglects terms of order $(\mu_R - \omega_M)/\omega_M$. Inserting $|\alpha_{j,1}|_{max}$ into Eq. (12) and assuming the exponent is small gives

$$P_{\uparrow,SM}^{(j)} \simeq \frac{1}{2}\left[2\left|\alpha_{j,1}\right|_{max}^2 (2\bar{n}_1 + 1))\right] . \tag{14}$$

We compare $P_{\uparrow,SS}^{(j)}$ (Eq. (13)) with $P_{\uparrow,SM}^{(j)}$ (Eq. (14)),

$$\frac{P_{\uparrow,SS}^{(j)}}{P_{\uparrow,SM}^{(j)}} \simeq \frac{N \cdot 8\,(Jt)^2}{2\left|\alpha_{j,1}\right|_{max}^2 (2\bar{n}_1 + 1)} \simeq \frac{F^2}{4\hbar^2} \cdot \frac{z_{01}^2}{2\bar{n}_1 + 1} t^2 . \tag{15}$$

For the work reported here $F \sim 10^{-23}$ N, $z_{01} = \sqrt{\hbar/(2M\omega_1)} \sim 30$ nm, and $\bar{n}_1 \sim 10$ (Doppler cooling limit). For a typical interaction time $t \lesssim 10^{-3}$ s we calculate $P_{\uparrow,SS}^{(j)}/P_{\uparrow,SM}^{(j)} \lesssim 0.1$. Therefore for small detunings satisfying $|\mu_R - \omega_1| \lesssim (2\pi)/t \ll \omega_1$ we expect the spin-motion entanglement signature generated by $\hat{U}_{SM}(t)$ to dominate contributions due to $\hat{U}_{SS}(t)$. We note that the spin-motion entanglement signature $\left(P_{\uparrow,SM}^{(j)}\right)$ decreases with decreasing temperature. For ground state cooling it may not be possible to neglect $\hat{U}_{SS}(t)$.

Expressions similar to Eq. (15) can be derived for small detunings of μ_R from an arbitrary mode m [6, 7]. Therefore, we expect that neglecting $\hat{U}_{SS}(t)$ when resonantly coupling to non-COM modes is a good approximation for the work reported here. We observe that this gives a good description of our experimental measurements for μ_R tuned close to the tilt (ω_2 and ω_3) and the next lower frequency modes (ω_4 and ω_5).

Spin Echo Sequence with Decoherence

To calculate $\alpha_{jm}(t)$ for the full spin echo sequence used in the experiment (see Fig. 4(b)), we must account for the accumulated phase difference between the ODF drive and oscillating ion cloud over the first arm and intermediate microwave π-pulse of combined duration $(\tau + t_\pi)$. This requires derivation of $\alpha_{jm}(t)$ for an ODF interaction with an arbitrary phase offset, ϕ, given by the more general

$$H_{ODF}(\phi) = -\sum_{j=1}^{N} F_j \cos\left(\mu_R t + \phi\right) \hat{z}_j \hat{\sigma}_j^z , \tag{16}$$

where $\phi = (\tau + t_\pi)(\mu_R - \omega_m) = (\tau + t_\pi)\delta_m$. Following the previous derivation of $\alpha_{jm}(t)$ for $\phi = 0$ (Eq. (8)), we obtain

$$\alpha_{jm}(t,\phi) = \frac{F_j b_{jm} z_{0m}}{\hbar\left(\mu_R^2 - \omega_m^2\right)}\left[\omega_m \cos(\phi) - i\mu_R \sin(\phi) - e^{i\omega_m t}\left\{\omega_m \cos(\mu_R t + \phi) - i\mu_R \sin(\mu_R t + \phi)\right\}\right] . \tag{17}$$

We now define a new $\alpha_{jm}^{\mathrm{SE}}$ that may be substituted for α_{jm} in Eq. (10) to calculate $P_\uparrow$ for the full spin echo sequence exhibiting arm durations of τ:

$$\alpha_{jm}^{\mathrm{SE}} = \alpha_{jm}(\tau, \phi = 0) - \alpha_{jm}(\tau, \phi), \tag{18}$$

where the above expression is given explicitly in Eq. (3) of the Letter.

To justify implementation of Eq. (18), it is useful to calculate $P_\uparrow$ for a single spin undergoing both the Ramsey and spin echo sequences. To simplify notation, we define the displacement operator $\hat{D}(\alpha_{jm}) = \exp(\alpha_{jm}\hat{a}_m^\dagger - \alpha_{jm}^*\hat{a}_m)$ which is applied separately to $|\uparrow_j\rangle \otimes |\psi_m\rangle$ and $|\downarrow_j\rangle \otimes |\psi_m\rangle$, where $|\psi_m\rangle$ is an arbitrary motional state of mode m. Assuming the state is initialized to $|\uparrow_j\rangle \otimes |\psi_m\rangle$, we calculate the result of the Ramsey sequence, $P_\uparrow^{(j)\mathrm{Ramsey}}$, to be

$$P_\uparrow^{(j)\mathrm{Ramsey}} = \frac{1}{4}\langle\psi_m|\left\{\hat{D}^\dagger\left(\alpha_{jm}(\tau,\phi)\right) - \hat{D}^\dagger\left(-\alpha_{jm}(\tau,\phi)\right)\right\}\{h.c.\}\,|\psi_m\rangle, \tag{19}$$

where $\{h.c.\}$ denotes the Hermitian conjugate of the first bracketed expression. Here the arbitrary phase ϕ has no physical significance since its value is common to all displacements, and we have once again made the assumption that $F_{j\uparrow} = -F_{j\downarrow}$. However, the spin echo result given by $P_\uparrow^{(j)\mathrm{SE}}$ is

$$\begin{aligned} P_\uparrow^{(j)\mathrm{SE}} &= \frac{1}{4}\langle\psi_m|\left\{\hat{D}^\dagger\left(-\alpha_{jm}(\tau,\phi)\right)\hat{D}^\dagger\left(\alpha_{jm}(\tau,0)\right) - \hat{D}^\dagger\left(\alpha_{jm}(\tau,\phi)\right)\hat{D}^\dagger\left(-\alpha_{jm}(\tau,0)\right)\right\}\{h.c.\}\,|\psi_m\rangle & (20)\\ &= \frac{1}{4}\langle\psi_m|\left\{\hat{D}^\dagger\left(\alpha_{jm}^{\mathrm{SE}}\right) - \hat{D}^\dagger\left(-\alpha_{jm}^{\mathrm{SE}}\right)\right\}\{h.c.\}\,|\psi_m\rangle. & (21)\end{aligned}$$

We obtain Eq. (21) from Eq. (20) using the multiplicative properties of $\hat{D}$ and neglecting overall phase factors that leave $P_\uparrow^{(j)\mathrm{SE}}$ unchanged. Note that Eq. (21) is identical to Eq. (19) after an appropriate redefinition of α_{jm}.

Finally, the derivation of Eq. (12) neglected the effects of spontaneous emission from the ODF laser beams. Decoherence of the Bloch vector due to spontaneous emission from off-resonant light is well studied in our system [8]. The qubit levels are closed under spontaneous light scattering; that is, spontaneous light scattering does not optically pump an ion to a different ground state level outside of the two qubit levels. In the presence of off-resonant laser light, the decrease in the Bloch vector due to spontaneous scattering during the arms of a spin-echo sequence is

$$P_{\uparrow,spon}^{(j)} = \frac{1}{2}\left[1 - \exp\left(-\Gamma \cdot 2\tau\right)\right] .$$

Here $\Gamma \equiv \left(\Gamma_{Ram} + \Gamma_{el}\right)/2$ has contributions from both Raman scattering and elastic Rayleigh scattering that can be calculated from the laser beam parameters. With the spin echo sequence, we account for spontaneous emission by modifying Eq. (12) as follows

$$P_{\uparrow,SM}^{(j)\mathrm{SE}} = \frac{1}{2}\left[1 - e^{-\Gamma 2\tau}\exp\left(-2\sum_m \left|\alpha_{jm}^{\mathrm{SE}}\right|^2\left(2\bar{n}_m + 1\right)\right)\right],$$

where τ is the length of time of a single arm of the spin-echo sequence.

[1] J. W. Britton et al. (2012), DOI: 10.1038/nature10981.
[2] S.-L. Zhu and Z. D. Wang, Phys. Rev. Lett. **91**, 187902 (2003).
[3] K. Kim, M.-S. Chang, R. Islam, S. Korenblit, L.-M. Duan, and C. Monroe, Phys. Rev. Lett. **103**, 120502 (2009).
[4] N. W. Ashcroft and N. D. Mermin, *Solid State Physics* (Saunders College, Philadelphia, 1976), p. 792.
[5] M. Kitagawa and M. Ueda, Phys. Rev. A **47**, 5138 (1993).
[6] D. Porras, private communication.
[7] M. Kastner, Phys. Rev. Lett. **106**, 130601 (2011).
[8] H. Uys, M. J. Biercuk, A. VanDevender, C. Ospelkaus, D. Meiser, R. Ozeri, and J. J. Bollinger, Phys. Rev. Lett. **105**, 200401 (2010).